SIAM J. SCI. COMPUT.
Vol. 39, No. 1, pp. B53–B75

PARTIAL OUTER CONVEXIFICATION FOR TRAFFIC LIGHT OPTIMIZATION IN ROAD NETWORKS*

SIMONE GÖTTLICH†, ANDREAS POTSCHKA‡, AND UTE ZIEGLER†

Abstract. We consider the problem of computing optimal traffic light programs for urban road intersections using traffic flow conservation laws on networks. Based on a partial outer convexification approach, which has been successfully applied in the area of mixed-integer optimal control for systems of ordinary or differential algebraic equations, we develop a computationally tractable two-stage solution heuristic. The two-stage approach consists of the solution of a (smoothed) nonlinear programming problem with dynamic constraints and a reconstruction mixed-integer linear program without dynamic constraints. The two-stage approach is founded on a discrete approximation lemma for partial outer convexification, whose grid-independence properties for (smoothed) conservation laws are investigated. We use the two-stage approach to compute traffic light programs for two scenarios on different discretizations and demonstrate that the solution candidates cannot be improved in a reasonable amount of time by global state-of-the-art mixed-integer nonlinear programming solvers. The two-stage solution candidates are not only better than results obtained by global optimization of piecewise linearized traffic flow models but also can be computed at a faster rate.

Key words. partial outer convexification, traffic networks, discretized conservation laws, optimization, mixed-integer programming

AMS subject classifications. 35L65, 49J20, 90C11, 90C35

DOI. 10.1137/15M1048197

1. Introduction.

With their seminal papers [22, 25] in the 1950s on time-dependent models for traffic flow with continuous densities instead of individual vehicles, Lighthill and Whitham and Richards established a new area of mathematical research in traffic modeling. The area is still highly active, e.g., for the case of traffic intersections (see, e.g., [5, 8]), which constitute a building block of larger road networks. Our goal in this paper is to devise efficient heuristics to approximately solve the problem of optimal traffic light settings for road networks. We base our work on the model and scenarios presented in [12] and refer the reader to the discussion therein for further references regarding the wide variety of different approaches for traffic light control or related problems such as spillover dissipation [11, 23].

The resulting mathematical optimization problems, which we elaborate in full detail in section 2, can be described as nonlinear mixed-integer optimal control problems constrained by scalar hyperbolic conservation laws on networks using boundary control. These problems are extremely challenging for several reasons: First, the problems are infinite dimensional in nature and must be discretized appropriately. Special care has to be exercised for the discretization of the scalar conservation laws in order to guarantee well-posedness and, on the discrete level, consistency and sta-

*Submitted to the journal's Computational Methods in Science and Engineering section November 12, 2015; accepted for publication (in revised form) October 31, 2016; published electronically February 1, 2017.

http://www.siam.org/journals/sisc/39-1/M104819.html

Funding: This work was supported by ERC Advanced Investigator grant MOBOCON (291 458) and by German Federal Ministry of Education and Research grant 05M2013.

†School of Business Informatics and Mathematics, University of Mannheim, 68131 Mannheim, Germany (goettlich@uni-mannheim.de, ziegler@uni-mannheim.de).

‡Interdisciplinary Center for Scientific Computing, Heidelberg University, 69120 Heidelberg, Germany (potschka@iwr.uni-heidelberg.de).

bility. Due to their combination of discrete and continuous variables, they are hybrid in nature, and on fine discretizations the combinatorial complexity of the feasible set is tremendous. In addition, the nonlinearities require sophisticated theoretical and numerical methods.

For nonlinear mixed-integer optimal control problems constrained by ordinary or differential algebraic equations, Sager, Bock, and Diehl [26] pioneered a partial outer convexification (POC) approach which yields strong theoretical results, including existence of feasible points with arbitrarily small integer optimality gap. The proofs are constructive and lend themselves directly to the formulation of a numerical method, which outperforms conventional branch-and-bound methods for mixed-integer nonlinear programming (MINLP) by several orders of magnitude on a test example; see [10, 20]. In [15], Hante and Sager extended the POC approach to mixed-integer optimal control problems constrained by semilinear evolution equations. Due to certain smoothness assumptions on the solution, these results cover partial differential equation (PDE) constraints of parabolic type. Recently, Hante [14] developed a POC theory for the case of mixed-integer optimal control problems constrained by first order semilinear hyperbolic systems in one space dimension with distributed control. His problem setting is close to our setting, but so far the generalization of his proof techniques to the case of boundary control seems to be out of reach, if not impossible.

The efficiency of the POC approach lies in its exploitation of the special pointwise nature of causality that the physical time imposes on the mixed-integer control decisions. For realistic solutions in traffic light control, however, we need to satisfy additional combinatorial constraints that tightly couple control decisions over certain time intervals, e.g., maximum red light and minimum green light phases. These constraints are only marginally addressed in [14], with a direct reference to the combinatorial integer approximation problem (CIAP) introduced by Sager, Jung, and Kirches [27]. In the presence of such coupling combinatorial constraints, the integer optimality gap in the POC approach can no longer be reduced to arbitrarily small values.

In this paper, we investigate how the heuristics based on the POC/CIAP approach compare, in terms of optimality and computational efficiency, with existing MINLP methods and linearization plus mixed-integer linear programming (MILP) methods. To this end, we first discretize the traffic light optimization problem appropriately and present a smoothing argument, which allows us to establish a time grid independent discrete POC approximation lemma. The constants we obtain, however, are not independent of the spatial discretization grid.

2. Problem formulation.

We first describe the road network traffic flow equations, which appear as constraints in the dynamic optimization problem to be described subsequently.

2.1. Traffic flow on road networks.

Coclite, Garavello, and Piccoli [5] proposed a model for traffic flow on road networks with one junction. A generalization to multijunction networks with traffic lights is straightforward (cf. [12]): We model the road network as a directed graph (V, E) with vertices $V = \{1, \dots, n_V\}$ as junctions and edges $E = \{1, \dots, n_E\}$ as unidirectional roads and denote the sets of incoming and outgoing roads of junctions $v \in V$ as $\delta_v^{\text{in}} \subset E$ and $\delta_v^{\text{out}} \subset E$. We partition the network vertices into three sets of incoming, outgoing, and inner junctions,

$$V^{\text{in}} = \{v \in V \,|\, \delta_v^{\text{in}} = \varnothing\}, \quad V^{\text{out}} = \{v \in V \,|\, \delta_v^{\text{out}} = \varnothing\}, \quad V^{\text{io}} = V \setminus \{V^{\text{in}} \cup V^{\text{out}}\}.$$

In addition, we denote the sets of incoming and outgoing roads of the network by

$$E^{\text{in}} = \{i \in E \,|\, \exists v \in V^{\text{in}} : i \in \delta_v^{\text{out}}\} \quad \text{and} \quad E^{\text{out}} = \{i \in E \,|\, \exists v \in V^{\text{out}} : i \in \delta_v^{\text{in}}\}.$$

Each road $i \in E$ has a given length $L_i > 0$. On the time horizon $[0, T]$ the road traffic densities $\rho_i(t, x) \in [0, \rho^{\max}]$, which we normalize to $\rho^{\max} = 1$ for the sake of simplicity and without loss of generality, satisfy for all $i \in E$ the one-dimensional hyperbolic conservation law

$$\partial_t \rho_i + \partial_x f(\rho_i) = 0 \quad \text{on } [0, T] \times [0, L_i], \tag{1}$$

where $f : [0, 1] \to \mathbb{R}$ is a nonnegative nonlinear continuous and piecewise twice continuously differentiable flow function with $f(0) = f(1) = 0$, a unique strict maximum at some $\rho^* \in (0, 1)$, and strict monotonicity on the intervals $(0, \rho^*)$ and $(\rho^*, 1)$. These assumptions guarantee the existence of a continuous function $\tau : [0, 1] \to [0, 1]$ with the properties $\tau(\rho) \neq \rho$ and $f(\rho) = f(\tau(\rho))$ for all $\rho \in [0, 1] \setminus \rho^*$. In many traffic flow applications [4, 24] a piecewise linear flow function (called triangular) is used. However, our focus is the consideration of a nonlinear flow function that will lead to a more challenging nonlinear mixed-integer problem. A piecewise linear flow function as in [12] will, however, play an important role in section 5.3 for a comparison of the performance of our proposed method with a heuristic based on MILP.

The densities must satisfy the given initial conditions

$$\rho_i(0, x) = \rho_i^0(x) \quad \text{for all } x \in [0, L_i],\ i \in E. \tag{2}$$

The prescribed spatial boundary conditions depend on the road network topology and on the current traffic light setting. On incoming roads of the network, we prescribe inhomogeneous Dirichlet inflow data

$$\rho_i(t, 0) = \rho_i^{\text{in}}(t) \quad \text{for all } t \in [0, T],\ i \in E^{\text{in}}. \tag{3}$$

On outgoing roads $i \in E^{\text{out}}$, free outflow is guaranteed by the omission of boundary conditions at $x = L_i$ for all $t \in [0, T]$. A detailed discussion on boundary conditions for roads going into the network (or outgoing roads, respectively) can be found in [3, 5]. We assume that all roads $i \in E \setminus E^{\text{out}}$ have a traffic light at $x = L_i$, whose setting at time $t \in [0, T]$ is denoted by $A_i(t) \in \{0, 1\}$, where 0 means red/stop and 1 means green/go. At red lights, the following no flow condition must hold:

$$f(\rho_i(t, L_i)) = 0 \quad \text{for all } t \in [0, T], i \in E \setminus E^{\text{out}} \text{ with } A_i(t) = 0. \tag{4}$$

For the sake of well-posedness of the Riemann problems at the inner junctions (see [5]) we need to require for all $t \in [0, T]$ and each inner vertex $v \in V^{\text{io}}$ the following relations to describe admissible boundary densities $\hat{\rho}_i(t)$, $i \in \delta_v^{\text{in}}$, and $\bar{\rho}_i(t)$, $i \in \delta_v^{\text{out}}$, and their corresponding fluxes $\hat{\gamma}_i(t)$, $i \in \delta_v^{\text{in}}$, and $\bar{\gamma}_i(t)$, $i \in \delta_v^{\text{out}}$:

$$\hat{\rho}_i(t) \in \begin{cases} \{\rho_i(t, L_i)\} \cup (\tau(\rho_i(t, L_i)), 1] & \text{if } \rho_i(t, L_i) \in [0, \rho^*] \\ [\rho^*, 1] & \text{otherwise} \end{cases} \quad \text{for } i \in \delta_v^{\text{in}}, \tag{5a}$$

$$\bar{\rho}_i(t) \in \begin{cases} [0, \rho^*] & \text{if } \rho_i(t, 0) \in [0, \rho^*] \\ \{\rho_i(t, 0)\} \cup [0, \tau(\rho_i(t, 0))) & \text{otherwise} \end{cases} \quad \text{for } i \in \delta_v^{\text{out}}, \tag{5b}$$

$$A_i(t)\hat{\gamma}_i(t) \leq \begin{cases} f(\rho_i(t, L_i)) & \text{if } \rho_i(t, L_i) \in [0, \rho^*] \\ f(\rho^*) & \text{otherwise} \end{cases} \quad \text{for } i \in \delta_v^{\text{in}}, \tag{5c}$$

$$\text{(5d)} \qquad \bar{\gamma}_i(t) \le \begin{cases} f(\rho^*) & \text{if } \rho_i(t,0) \in [0,\rho^*] \\ f(\rho_i(t,0)) & \text{otherwise} \end{cases} \qquad \text{for } i \in \delta_v^{\text{out}}.$$

In contrast to the usual notation, we use $A_i(t)\hat{\gamma}_i(t)$ in place of $\hat{\gamma}_i(t)$ in order to make the usually implicit dependence of $\hat{\gamma}_i(t)$ on $A_i(t)$ explicit (cf., e.g., [12]) because this reformulation dramatically improves the performance of the solvers for the Stage I problem introduced in section 4. Moreover, we require the Rankine–Hugoniot relation for the conservation of traffic,

$$\text{(6)} \qquad \sum_{j \in \delta_v^{\text{out}}} \bar{\gamma}_j(t) = \sum_{i \in \delta_v^{\text{in}}} A_i(t)\hat{\gamma}_i(t) \quad \text{for all } t \in [0,T],\ v \in V^{\text{io}}.$$

In order to guarantee unique solvability of the so far still underdetermined Riemann problems at inner junctions, we require the following two additional conditions (7) and (8): We model the vehicles' turning preferences with an $n_E \times n_E$ traffic distribution matrix, whose entries $d_{ij} \in [0,1]$ describe the fraction of traffic turning from road i into road j according to

$$\text{(7)} \qquad \bar{\gamma}_j(t) = \sum_{i \in \delta_v^{\text{in}}} d_{ij} A_i(t)\hat{\gamma}_i(t) \quad \text{for all } t \in [0,T],\ j \in \delta_v^{\text{out}}, v \in V^{\text{io}}.$$

For consistency with (6), the matrix entries must satisfy

$$\sum_{j \in \delta_v^{\text{out}}} d_{ij} = 1 \quad \text{for all } i \in \delta_v^{\text{in}},\ v \in V^{\text{io}}.$$

Finally, we assume that the traffic distributes itself at the inner junctions in a way that maximizes the junction traffic flows,

$$\text{(8)} \qquad \max \sum_{i \in \delta_v^{\text{out}}} \bar{\gamma}_i(t) \quad \text{for all } t \in [0,T],\ v \in V^{\text{io}},$$

which, due to (6), is equivalent to maximizing the sum of the terms $A_i(t)\hat{\gamma}_i(t)$ for $i \in \delta_v^{\text{in}}$, $v \in V^{\text{io}}$, as usually stated (cf., e.g., [12]). Equations (1)–(8) completely describe the traffic flow dynamics.

2.2. Traffic light optimization. For a given road network, we want to determine traffic light programs that maximize the cumulative traffic flow within the network. In realistic situations, further combinatorial constraints must be respected, e.g., logical implications of light configurations to avoid colliding crosstraffic at junctions, but possibly also bounds on the minimum green light or maximum red light phase durations.

The traffic light optimization problem can be cast in the form

$$\text{(9)} \qquad \max_{\substack{A_i:[0,T]\to\{0,1\},i\in E\setminus E^{\text{out}} \\ \rho_i:[0,T]\times[0,L_i]\to[0,1],i\in E}} \sum_{i\in E} \int_0^T \int_0^{L_i} f(\rho_i(t,x))\mathrm{d}x\mathrm{d}t + \sum_{i\in E\setminus E^{\text{in}}} \int_0^T \bar{\gamma}_i(t)\mathrm{d}t$$
$$\text{subject to} \qquad \text{(1)–(8) and additional combinatorial constraints.}$$

Another way of posing problem (9) makes use of a disjunctive programming viewpoint [2] and paves the way for the application of POC in section 3.4. To this end, we enumerate all feasible traffic light configurations at a time $t \in [0,T]$ in a set

$\Omega := \{a^1, \dots, a^{n_\Omega}\}$ of binary vectors $a^j \in \{0,1\}^{n_E}$ for $j = 1, \dots, n_\Omega$. The number n_Ω of elements in Ω is at most 2^{n_E}. At this point, infeasible configurations with red lights at the end of outgoing roads or with violations of other time-independent logical implications can already be removed from Ω so that $n_\Omega \ll 2^{|E \setminus E^{\text{out}}|}$, e.g., $n_\Omega = 16 \ll 2^8$ as in the large intersection example with eight traffic lights in section 5. At each time $t \in [0,T]$ exactly one traffic light configuration is active, which we denote by a binary function $\omega : [0,T] \to \{0,1\}^{n_\Omega}$ that satisfies for $j = 1, \dots, n_\Omega$ the relation

$$\omega_j(t) = 1 \quad \Leftrightarrow \quad A_i(t) = a_i^j \quad \text{for all } i = 1, \dots, n_E.$$

The optimization problem (9) can now equivalently be stated as

(10)

$$\max_{\substack{\omega:[0,T]\to\{0,1\}^{n_\Omega} \\ \rho_i:[0,T]\times[0,L_i]\to[0,1], i\in E}} \sum_{i\in E} \int_0^T \int_0^{L_i} f(\rho_i(t,x))\mathrm{d}x\mathrm{d}t + \sum_{i\in E\setminus E^{\text{in}}} \int_0^T \bar{\gamma}_i(t)\mathrm{d}t$$

subject to (1)–(8) without (4),

$$\bigvee_{s=1}^{n_\Omega} \left[\begin{array}{c} \omega_s(t) = 1 \\ f(\rho_i(t,L_i)) = 0 \quad \text{for all } i \in E : a_i^s = 0 \end{array} \right] \quad \text{for all } t \in [0,T],$$

and additional combinatorial constraints coupling over time,

where the logical operator $\bigvee_{s=1}^{n_\Omega}$ implies that exactly one of the n_Ω logical terms in brackets is true at each time $t \in [0,T]$.

The main challenges of solving problems (9) and (10) are fourfold: First, the optimization variables and dynamic equations are temporally and spatially distributed on a complex network and must be discretized with care to properly capture the hyperbolic traffic dynamics, which include shock formations and rarefaction waves. Second, the resulting problems will be of large scale and thus require the use of sophisticated algorithms and computational machinery. Third, the problems contain binary decision variables and are thus of combinatorial nature. Fourth, the objective and constraints are nonlinear and nonconvex. Hence, efficient off-the-shelf methods from MILP cannot be applied as such. All four challenges alone constitute highly active areas of current research. The combination of the above four difficulties renders problems (9) and (10) especially hard.

As a first step towards the numerical solution of (10), we develop a two-phase heuristic method, which computes integer-feasible discretizations $\boldsymbol{\omega}_t$ of the multiplier functions ω. In the two-phase heuristic, we drop the constraint (8) in this paper for reasons explained in section 3.1. For the comparison of the achieved objective values in section 5, however, we take (8) into account through another simulation of the full forward dynamics using the heuristically obtained ω_t.

3. Discretization. We want to approximate problem (10) with a finite dimensional optimization problem. To this end, we discretize for each road $i \in E$ the traffic densities ρ_i on an equidistant Cartesian grid with (for simplicity) uniform time steps $\Delta t > 0$ and spatial mesh size of $\Delta x^{(i)} > 0$ uniformly on each road. We assume that $n_T = T/\Delta t$ and $n_L^i = L_i/\Delta x^{(i)}$ are integer for all $i \in E$ and set

$$\rho_{t,k}^i = \rho_i(t\Delta t, k\Delta x^{(i)}) \quad \text{for } i \in E,\ t = 0, \dots, n_T,\ k = 0, \dots, n_L^i.$$

We use the same staggered Lax–Friedrichs (sLxF) method as in [12] for the discretization of (1) (only the presentation chosen here differs slightly in order to

facilitate the use within POC). Compared to the standard Lax–Friedrichs method, the staggered method is less diffusive and can be implemented in a straightforward way, since boundary values are directly given in terms of the fluxes $\hat{\gamma}_t^i$ and $\bar{\gamma}_t^i$. To describe the traffic flow at the junctions regarding (5), we introduce for $t = 0, \dots, n_T - 1$ the temporally distributed real variables

$$\hat{\gamma}_t^i, \hat{h}_t^i \text{ for } i \in E \setminus E^{\text{out}} \quad \text{and} \quad \bar{\gamma}_t^i, \bar{h}_t^i \text{ for } i \in E \setminus E^{\text{in}}.$$

For all $t = 0, \dots, n_T$ the densities $\rho_{t,k}^i$ for $k \in \{-1, n_L^i + 1\}$, $i \in E$, the variables $\hat{\gamma}_t^i$ and $\hat{h}_t^i$ for $i \in E^{\text{out}}$, and the variables $\bar{\gamma}_t^i$ and $\bar{h}_t^i$ for $i \in E^{\text{in}}$ play the roles of ghost states and shall be specified below. For ease of notation, we introduce the column vectors

$$\begin{aligned}
&&\boldsymbol{\rho}_t &= \left(\left(\rho_{t,k}^i\right)_{k=0}^{n_L^i} \right)_{i \in E} && \text{for } t = 0, \dots, n_T,\\
\hat{\boldsymbol{\gamma}}_t &= \left(\hat{\gamma}_t^i\right)_{i \in E \setminus E^{\text{out}}}, & \bar{\boldsymbol{\gamma}}_t &= \left(\bar{\gamma}_t^i\right)_{i \in E \setminus E^{\text{in}}} && \text{for } t = 0, \dots, n_T - 1,\\
\hat{\boldsymbol{h}}_t &= \left(\hat{h}_t^i\right)_{i \in E \setminus E^{\text{out}}}, & \bar{\boldsymbol{h}}_t &= \left(\bar{h}_t^i\right)_{i \in E \setminus E^{\text{in}}} && \text{for } t = 0, \dots, n_T - 1.
\end{aligned}$$

3.1. Dynamic constraints. For the moment, let the traffic light configuration be fixed to a^s for some $s \in \Omega$. The sLxF scheme can then be formulated as

$$\begin{aligned}
\rho_{t+1,k}^i = \frac{\rho_{t,k-1}^i + 2\rho_{t,k}^i + \rho_{t,k+1}^i}{4} \\
- \frac{\Delta t}{2\Delta x^{(i)}} \left(f_{s,i,k}^+(\rho_{t,k+1}^i, \rho_{t,k}^i, \hat{\gamma}_t^i) - f_{s,i,k}^-(\rho_{t,k}^i, \rho_{t,k-1}^i, \bar{\gamma}_t^i) \right)
\end{aligned} \tag{11}$$

for $i \in E, t = 0, \dots, n_T - 1$, and $k = 0, \dots, n_L^i$, with numerical flux functions

$$f_{s,i,k}^+(\rho_+, \rho_\circ, \hat{\gamma}) = \begin{cases} 2a_i^s \hat{\gamma} - f(\rho_\circ) & \text{for } k = n_L^i,\ i \in E \setminus E^{\text{out}}, \\ 2f(\rho_\circ) & \text{for } k = n_L^i,\ i \in E^{\text{out}}, \\ f(\rho_+) & \text{otherwise,} \end{cases}$$

$$f_{s,i,k}^-(\rho_\circ, \rho_-, \bar{\gamma}) = \begin{cases} 2\bar{\gamma} - f(\rho_\circ) & \text{for } k = 0,\ i \in E \setminus E^{\text{in}}, \\ 2f(\rho_-) & \text{for } k = n_L^i,\ i \in E^{\text{in}}, \\ f(\rho_-) & \text{otherwise.} \end{cases}$$

We immediately observe that *only* f^+ depends on s through the occurrence of a_i^s in the first case.

For $t = 0, \dots, n_T - 1$ we now define the ghost states implicitly to incorporate the boundary conditions (3) and (4) and the free outflow conditions at outgoing edges according to

$$\begin{aligned}
\rho_{t,-1}^i &= \begin{cases} \rho_i^{\text{in}}(t\Delta t) & \text{for } i \in E^{\text{in}}, \\ \rho_{t,0}^i & \text{for } i \in E \setminus E^{\text{in}}, \end{cases} \qquad \rho_{t,n_L^i+1}^i = \begin{cases} \rho_{t,n_L^i-1}^i & \text{for } i \in E^{\text{out}}, \\ \rho_{t,n_L^i}^i & \text{for } i \in E \setminus E^{\text{out}}, \end{cases} \\
\bar{\gamma}_t^i &= f(\rho_i^{\text{in}}(t\Delta t)) \quad \text{for } i \in E^{\text{in}}, \qquad \hat{\gamma}_t^i = 0 \quad \text{for } i \in E^{\text{out}}.
\end{aligned} \tag{12}$$

The fluxes $\hat{\boldsymbol{\gamma}}_t, \bar{\boldsymbol{\gamma}}_t, \hat{\boldsymbol{h}}_t, \bar{\boldsymbol{h}}_t$ are determined via conditions (5c)–(5d) which require for $t = 0, \dots, n_T - 1$

$$\hat{\gamma}_t^i \le f(\min(\rho_{t,n_L^i}^i, \rho^*)) \text{ for } i \in E \setminus E^{\text{out}} \quad \text{and} \quad \bar{\gamma}_t^i \le f(\max(\rho_{t,0}^i, \rho^*)) \text{ for } i \in E \setminus E^{\text{in}},$$

which we bring to a differentiable formulation

$$\begin{aligned} &\hat{\gamma}_t^i \le f(\hat{h}_t^i), \quad \hat{h}_t^i \le \rho^*, \quad \hat{h}_t^i \le \rho_{t,n_L^i}^i \quad \text{for } i \in E \setminus E^{\text{out}}, \\ &\bar{\gamma}_t^i \le f(\bar{h}_t^i), \quad \bar{h}_t^i \ge \rho^*, \quad \bar{h}_t^i \ge \rho_{t,0}^i \quad \text{for } i \in E \setminus E^{\text{in}} \end{aligned} \tag{13}$$

via the slack variables

$$\hat{h}_t^i = \min(\rho_{t,n_L^i}^i, \rho^*) \text{ for } i \in E \setminus E^{\text{out}} \quad \text{and} \quad \bar{h}_t^i = \max(\rho_{t,0}^i, \rho^*) \text{ for } i \in E \setminus E^{\text{in}}.$$

The junction entropy condition (8) in discretized form reads

$$\max \sum_{i \in \delta_v^{\text{out}}} \bar{\gamma}_t^i \quad \text{for all } v \in V, t = 0, \dots, n_T - 1. \tag{14}$$

We remark here that we shall later drop the requirement (14) (and thus (8)) in order to avoid a bilevel optimization problem (see, e.g., [7, 6]) with n_T lower level problems in the first stage of the two-stage approach outlined in section 4. In comparison, the bilevel approach would yield a stronger approximation result, but at the expense of a much more challenging numerical approach for the nonlinear optimization problem needed to be solved in the first stage of the algorithm we propose.

In order to describe the traffic distribution at junctions, we can now discretize (7) as

$$\bar{\gamma}_t^j = \sum_{i \in \delta_v^{\text{in}}} d_{ij} a_j^s \hat{\gamma}_s^i \quad \text{for all } t = 0, \dots, n_T - 1,\ j \in \delta_v^{\text{out}}, v \in V^{\text{io}}.$$

Finally, we assume that the initial conditions for the densities are provided in $\rho_{0,k}^i$ for $i \in E$, $k = 0, \dots, n_L^i$. This completes the discretization of the traffic flow equations as differentiable dynamic constraints. We remark here that for numerical stability, the discretization grid must satisfy the Courant–Friedrichs–Lewy (CFL) condition

$$C_{\text{CFL}} \Delta t \le \Delta x^{(i)} \quad \text{for all } i \in E, \tag{15}$$

where $C_{\text{CFL}} = 2 \|f'\|_\infty$ depends on the maximum norm of the derivative $f' : [0, 1] \to \mathbb{R}$ of the flow function. In addition, it is necessary for the convergence of the sLxF scheme that an inverse CFL condition of the form

$$\Delta x^{(i)} \le c \Delta t \quad \text{for some constant } c > 0 \tag{16}$$

is satisfied (cf. section 3.2).

3.2. Decoupling of temporal and spatial discretization. At the end of section 4.1 we shall discuss approximation properties, which require that Δt can be made arbitrarily small in comparison to $\Delta x^{(i)}, i \in E$, so that the inverse CFL condition (16) cannot hold. The sLxF method achieves its simplicity by introduction of an artificial diffusion term in (1) according to

$$\partial_t \rho_i + \partial_x f(\rho_i) = \nu^{(i)} \partial_{xx} \rho_i \quad \text{on } [0, T] \times [0, L_i],\ i \in E, \tag{17}$$

for some small $\nu^{(i)} > 0,\ i \in E$. If we apply standard finite differences to the parabolic equation (17), we obtain

$$\begin{aligned} \rho_{t+1,k}^i = \rho_{t,k}^i &+ \nu^{(i)} \Delta t \frac{\rho_{t,k-1}^i - 2\rho_{t,k}^i + \rho_{t,k+1}^i}{(\Delta x^{(i)})^2} \\ &- \frac{\Delta t}{2\Delta x^{(i)}} (f_{s,i,k}^+(\rho_{t,k+1}^i, \rho_{t,k}^i, \hat{\gamma}_t^i) - f_{s,i,k}^-(\rho_{t,k}^i, \rho_{t,k-1}^i, \bar{\gamma}_t^i)) \end{aligned} \tag{18}$$

for $i \in E,\ t = 0, \dots, n_T - 1$, and $k = 0, \dots, n_L^i$. With the choice

$$\nu^{(i)} = (\Delta x^{(i)})^2/(4\Delta t), \tag{19}$$

we recover the sLxF scheme (11) for the hyperbolic equation (1). As we observe, the coefficient $\nu^{(i)}$ of the diffusion terms depends on the chosen discretization. The inverse CFL condition (16) ensures that $\nu^{(i)} \to 0$ as $\Delta t \to 0$. In contrast, if $\Delta x^{(i)}$ stays bounded away from 0, then $\nu^{(i)} \to \infty$ as $\Delta t \to 0$, and the traffic flow dynamics are completely overpowered by the strong diffusion term. Thus, the decoupling of $\Delta x^{(i)}$ and Δt by fixing $\nu^{(i)}$ allows us to let Δt go to zero. The scheme (18) will then converge to a solution of the parabolic variant with artificial diffusion (17) of the original conservation law (1). At the end of section 4.1 we shall discuss approximation properties of mixed-integer relaxations only for the parabolic version and not the original problem.

We perform all further analysis in the setting of (17) and (18) with fixed $\nu^{(i)}$ (independent of Δt and $\Delta x^{(i)}$) instead of (1) and (11), knowing that (11) and (18) coincide for the choice (19).

After substitution of the ghost states (12) in (18), we arrive at the vectorial short form

$$\boldsymbol{\rho}_{t+1} = \boldsymbol{\rho}_t + \Delta t \Phi^s(t, \boldsymbol{\rho}_t, \hat{\boldsymbol{\gamma}}_t, \bar{\boldsymbol{\gamma}}_t, \hat{\boldsymbol{h}}_t, \bar{\boldsymbol{h}}_t) \quad \text{for } t = 0, \dots, n_T - 1, \tag{20}$$

where the function Φ^s depends on the current traffic light configuration a^s.

In order to obtain useful traffic light programs, we have to enforce further constraints in practice. As in [12], we consider upper time limits on red phases and lower limits on green phases. We defer their exact formulation until section 4.2. These constraints impose an additional combinatorial complexity on the traffic light optimization problem, because in their presence the control decisions are tightly coupled over whole time intervals. This property leads to detrimental effects in the application of the POC approach; see sections 3.4 and 4.

3.3. Discretized optimization problem. In order to provide a complete description of the discretized optimization problem in disjunctive form, we also discretize the binary function $\omega(t)$ on the time grid, denoted by

$$\boldsymbol{\omega}_t = (\omega_t^s)_{s=1}^{n_\Omega} \in \{0,1\}^{n_\Omega} \quad \text{for } t = 0, \dots, n_T - 1.$$

We finally arrive at the large-scale mixed-integer nonlinear optimization problem

(21)

$$\max_{\substack{\boldsymbol{\omega}_t, \hat{\boldsymbol{\gamma}}_t, \bar{\boldsymbol{\gamma}}_t, \hat{\boldsymbol{h}}_t, \bar{\boldsymbol{h}}_t, \\ t=0,\dots,n_T-1, \\ \boldsymbol{\rho}_t, t=1,\dots,n_T}} \sum_{i \in E} \sum_{t=1}^{n_T} \sum_{k=0}^{n_L^i} f(\rho_{t,k}^i) \Delta x^{(i)} \Delta t + \sum_{i \in E \setminus E^{\text{in}}} \sum_{t=0}^{n_T-1} \bar{\gamma}_t^i \Delta t$$

$$\text{subject to } \bigvee_{s=1}^{n_\Omega} \begin{bmatrix} \omega_t^s = 1 \\ \boldsymbol{\rho}_{t+1} = \boldsymbol{\rho}_t + \Delta t \Phi^s(t, \boldsymbol{\rho}_t, \hat{\boldsymbol{\gamma}}_t, \bar{\boldsymbol{\gamma}}_t, \hat{\boldsymbol{h}}_t, \bar{\boldsymbol{h}}_t) \\ \bar{\gamma}_t^j = \sum_{i \in \delta_v^{\text{in}}} d_{ij} a_j^s \hat{\gamma}_s^i \quad \text{for all } j \in \delta_v^{\text{out}}, v \in V^{\text{io}} \end{bmatrix} \text{ for all } t = 0, \dots, n_T - 1,$$

$$\hat{\gamma}_t^i \le f(\hat{h}_t^i), \hat{h}_t^i \le \rho^*, \hat{h}_t^i \le \rho_{t,n_L^i}^i \quad \text{for all } i \in E \setminus E^{\text{out}},\ t = 0, \dots, n_T - 1,$$

$$\bar{\gamma}_t^i \le f(\bar{h}_t^i), \bar{h}_t^i \ge \rho^*, \bar{h}_t^i \ge \rho_{t,0}^i \quad \text{for all } i \in E \setminus E^{\text{in}},\ t = 0, \dots, n_T - 1,$$

and additional combinatorial constraints coupling over time.

We consider the MINLP formulation (21) in the remainder of this paper.

3.4. Partial outer convexification. The disjunctive formulation of problem (21) can be transformed into a conventional MINLP formulation by the use of convex combinations, where the entries of $\boldsymbol{\omega}_t$ serve as convex multipliers. If the integrality condition on $\boldsymbol{\omega}_t$ is kept, problem (21) can be equivalently cast as

(22)

$$\max_{\substack{\boldsymbol{\omega}_t,\hat{\boldsymbol{\gamma}}_t,\bar{\boldsymbol{\gamma}}_t,\hat{\boldsymbol{h}}_t,\bar{\boldsymbol{h}}_t,\\ t=0,\dots,n_T-1,\\ \boldsymbol{\rho}_t,t=1,\dots,n_T}} \sum_{i\in E}\sum_{t=1}^{n_T}\sum_{k=0}^{n_L^i} f(\rho_{t,k}^i)\Delta x^{(i)}\Delta t + \sum_{i\in E\setminus E^{\mathrm{in}}}\sum_{t=0}^{n_T-1}\bar{\gamma}_t^i\Delta t$$

$$\text{subject to}\quad \left.\begin{aligned} &\sum_{s=1}^{n_\Omega}\omega_t^s = 1\\ &\boldsymbol{\rho}_{t+1} = \boldsymbol{\rho}_t + \Delta t\boldsymbol{\Phi}(t,\boldsymbol{\rho}_t,\hat{\boldsymbol{\gamma}}_t,\bar{\boldsymbol{\gamma}}_t,\hat{\boldsymbol{h}}_t,\bar{\boldsymbol{h}}_t)\boldsymbol{\omega}_t\\ &\bar{\gamma}_t^j = \sum_{s=1}^{n_\Omega}\sum_{i\in\delta_v^{\mathrm{in}}} d_{ij}a_j^s\hat{\gamma}_s^i\omega_t^s \quad \text{for all } j\in\delta_v^{\mathrm{out}}, v\in V^{\mathrm{io}}\\ &\hat{\gamma}_t^i \le f(\hat{h}_t^i), \hat{h}_t^i \le \rho^*, \hat{h}_t^i \le \rho_{t,n_L^i}^i \quad \text{for all } i\in E\setminus E^{\mathrm{out}}\\ &\bar{\gamma}_t^i \le f(\bar{h}_t^i), \bar{h}_t^i \ge \rho^*, \bar{h}_t^i \ge \rho_{t,0}^i \quad \text{for all } i\in E\setminus E^{\mathrm{in}} \end{aligned}\right\} \text{for all } t=0,\dots,n_T-1,$$

and additional combinatorial constraints coupling over time,

where the sth column of the matrix-valued function $\boldsymbol{\Phi}$ is constituted by the function Φ^s for $s=1,\dots,n_\Omega$ from (20).

4. Computation of near-optimal solutions. The aim of this paper is to devise a fast heuristic for approximate solutions of (9) via the generation of feasible points of (22) with near-optimal objective value. We follow the approach in [27, 18, 19] and split the solution of the mixed-integer nonlinear program (22) into two stages. Stage I comprises the solution of one nonlinear program, and Stage II comprises the solution of one mixed-integer linear program without dynamic constraints in which the solution of Stage I enters as data.

Our computational approach can be outlined in the following steps:

1. **Discretize** by choosing suitable spatial mesh sizes $\Delta x^{(i)} > 0,\ i\in E$. Relax problem by omitting (14).
2. **Smooth** the dynamics by determining the maximal CFL-compatible sLxF time step Δt_{CFL} to define the artificial diffusion coefficients
$$\nu^{(i)} = \frac{(\Delta x^{(i)})^2}{4\Delta t_{\mathrm{CFL}}} = \frac{(\Delta x^{(i)})^2}{4\min_{j\in E}\frac{\Delta x^{(j)}}{2\|f'\|_\infty}} = \frac{\|f'\|_\infty(\Delta x^{(i)})^2}{2\min_{j\in E}\Delta x^{(j)}},\quad i\in E.$$
Initialize $\Delta t = \Delta t_{\mathrm{CFL}}$.
3. Stage I: **Relax** the integrality condition
$$\boldsymbol{\omega}_t\in\{0,1\}^{n_\Omega} \quad\rightsquigarrow\quad \boldsymbol{\omega}_t\in[0,1]^{n_\Omega}$$
for $t=0,\dots,n_T-1$ in the partially outer convexified problem (22) and solve the resulting continuous nonlinear program to obtain an optimal vector $(\boldsymbol{\omega}_t^{\mathrm{rlx}})_{t=0}^{n_T-1}$.
4. Stage II: **Reconstruct** a binary feasible vector $(\boldsymbol{\omega}_t^{\mathrm{bin}})_{t=0}^{n_T-1}$ as the solution of the CIAP, a mixed-integer linear program without dynamic constraints in which $(\boldsymbol{\omega}_t^{\mathrm{rlx}})_{t=0}^{n_T-1}$ enters as data (see (28) in section 4.1).
5. **Simulate** the traffic dynamics again with $(\boldsymbol{\omega}_t^{\mathrm{bin}})_{t=0}^{n_T-1}$ to obtain a feasible trajectory and a corresponding objective value.

Optionally, a refinement step of the temporal mesh size Δt can be performed after step 4 to improve the accuracy of the switching if necessary, but this step is only useful in the case without additional combinatorial constraints that couple over time [26, 27]. We do not consider this option in the numerical computations in this paper. However, temporal mesh refinement is important for the discussion of approximation properties at the end of section 4.1.

We first discuss the case in which no additional combinatorial constraints that couple over time, e.g., bounds on the minimal and maximal red and green phases of each traffic light, are present. In this case, we can give a rigorous bound on the quality of the heuristic.

4.1. Case I: No combinatorial constraints that couple over time. The idea for the construction of the nonlinear program is simply the relaxation of the integrality condition $\boldsymbol{\omega}_t \in \{0,1\}^{n_\Omega}$ to $\boldsymbol{\omega}_t \in [0,1]^{n_\Omega}$ for $t = 0, \dots, n_T - 1$. The following approximation lemma is the reason why we study the optimization problem in the form (22) and not in a form which contains direct discretizations of the binary traffic light control $A(t)$ like in (9), for which no equally strong relaxation results are known to the authors.

The lemma is a discrete version of [26, Theorem 2]. Another discrete version exists [17], and we point out the differences below. In order to state the lemma, we need the convex hull of the columns of the identity matrix

$$\mathcal{H} = \left\{ \alpha \in \mathbb{R}^{n_\Omega}_{\geq 0} \;\middle|\; \sum_{i=1}^{n_\Omega} \alpha_i = 1 \right\}$$

and two norms $\|.\|_X : \mathbb{R}^n \to \mathbb{R}_{\geq 0}$ and $\|.\|_\Omega : \mathbb{R}^{n_\Omega} \to \mathbb{R}_{\geq 0}$.

LEMMA 1. *Let $I = \{0, \dots, n_T - 1\}, D \subseteq \mathbb{R}^n$, and $\Phi : I \times D \to \mathbb{R}^{n \times n_\Omega}$ be a matrix-valued function that is continuous with respect to the second argument and satisfies*

$$\|\Phi(t,y)v\|_X \leq M \|v\|_\Omega \qquad \text{for all } t \in I, y \in D, v \in \mathbb{R}^{n_\Omega}, \tag{23}$$

$$\|[\Phi(t,y) - \Phi(t,\eta)]\,\alpha\|_X \leq L \|y - \eta\|_X \qquad \text{for all } t \in I, y, \eta \in D, \alpha \in \mathcal{H} \tag{24}$$

for constants $M, L < \infty$. Furthermore, for each $t \in I$ let $h_t > 0, \alpha^t, \beta^t \in \mathcal{H}$ such that $T = \sum_{t=0}^{n_T-1} h_t$, and for each $t \in I \cup \{n_T\}$ let $y^t, \eta^t \in D$ be given such that for all $t \in I$

$$y^{t+1} = y^t + h_t \Phi(t, y^t)\alpha^t \qquad \text{and} \qquad \eta^{t+1} = \eta^t + h_t \Phi(t, \eta^t)\beta^t.$$

If for some set $I' \subseteq I$, constants $C, \varepsilon < \infty$, and some vector $\delta^0 \in \mathbb{R}^{n_\Omega}$ it holds that

$$\left\| \left[\Phi(t+1, y^{t+1}) - \Phi(t, y^t)\right] v \right\|_X \leq h_t C \|v\|_\Omega \qquad \text{for all } t \in I', v \in \mathbb{R}^{n_\Omega}, \tag{25}$$

$$\left\| \delta^0 + \sum_{t=0}^{k-1} h_t(\alpha^t - \beta^t) \right\|_\Omega \leq \varepsilon \qquad \text{for all } k \in I \cup \{n_T\}, \tag{26}$$

then it follows with $T'_k = k \max\{h_t \,|\, t = 0, \dots, k-1\}$ and $n_{\text{jump}} = |I \setminus (I' \cup \{n_T - 1\})|$ that for all $k \in I \cup \{n_T\}$

$$\sum_{t=0}^{k} h_t \left\| y^t - \eta^t \right\|_X \leq \frac{\exp(T'_k L) - 1}{L} \left(\left\| y^0 - \eta^0 \right\|_X + (2M(1 + n_{\text{jump}}) + TC)\varepsilon \right).$$

Proof. For $k \in I \cup \{n_T\}$, we define

$$e^k = y^k - \eta^k \quad \text{and} \quad \delta^k = \delta^0 + \sum_{t=0}^{k-1} h_t(\alpha^t - \beta^t).$$

We immediately obtain

(27)

$$\begin{aligned}
\left\|e^k\right\|_X &= \left\| y^0 + \sum_{t=0}^{k-1} h_t \Phi(t, y^t)\alpha^t - \eta^0 - \sum_{t=0}^{k-1} h_t \Phi(t, \eta^t)\beta^t \right\|_X \\
&= \left\| (y^0 - \eta^0) + \sum_{t=0}^{k-1} h_t \Phi(t, y^t)(\alpha^t - \beta^t) + \sum_{t=0}^{k-1} h_t \left(\Phi(t, y^t) - \Phi(t, \eta^t)\right)\beta^t \right\|_X \\
&\le \left\|e^0\right\|_X + \left\| \sum_{t=0}^{k-1} \Phi(t, y^t) h_t(\alpha^t - \beta^t) \right\|_X + \left\| \sum_{t=0}^{k-1} h_t \left(\Phi(t, y^t) - \Phi(t, \eta^t)\right)\beta^t \right\|_X .
\end{aligned}$$

We use Abel summation (the discrete version of integration by parts) and assumptions (23), (25), and (26) to bound the penultimate term in (27) according to

$$\begin{aligned}
&\left\| \sum_{t=0}^{k-1} \Phi(t, y^t) h_t(\alpha^t - \beta^t) \right\|_X = \left\| \sum_{t=0}^{k-1} \Phi(t, y^t)(\delta^{t+1} - \delta^t) \right\|_X \\
&= \left\| \Phi(k-1, y^{k-1})\delta^k - \Phi(0, y^0)\delta^0 - \sum_{t=0}^{k-2} \left[\Phi(t+1, y^{t+1}) - \Phi(t, y^t)\right] \delta^{t+1} \right\|_X \\
&\le \left\|\Phi(k-1, y^{k-1})\delta^k\right\|_X + \left\|\Phi(0, y^0)\delta^0\right\|_X + \sum_{t=0}^{k-2} \left\| \left[\Phi(t+1, y^{t+1}) - \Phi(t, y^t)\right] \delta^{t+1} \right\|_X \\
&\le (2M + TC + 2Mn_{\text{jump}})\varepsilon,
\end{aligned}$$

where we have split up the last occurring sum over indices in I' (sum $\le TC\varepsilon$) and not in I' (sum $\le 2Mn_{\text{jump}}\varepsilon$). Using (24), the third term in (27) can be bounded as

$$\left\| \sum_{t=0}^{k-1} h_t \left[\Phi(t, y^t) - \Phi(t, \eta^t)\right] \beta^t \right\|_X \le L \sum_{t=0}^{k-1} h_t \left\|e^t\right\|_X .$$

We finally obtain

$$\left\|e^k\right\|_X \le \left\|e^0\right\|_X + (2M(1 + n_{\text{jump}}) + TC)\varepsilon + L \sum_{t=0}^{k-1} h_t \left\|e^t\right\|_X ,$$

which is equivalent to

$$\frac{B^{k+1} - B^k}{h_k} \le \left\|e^0\right\|_X + (2M(1 + n_{\text{jump}}) + TC)\varepsilon + LB^k, \quad \text{where } B^k = \sum_{t=0}^{k-1} h_t \left\|e^t\right\|_X ,$$

which implies with $h_k^{\max} = \max\{h_t \,|\, t = 0, \ldots, k\}$ for all $i \le k$ that

$$B^{i+1} \le h_k^{\max} \left\|e^0\right\|_X + h_k^{\max}(2M(1 + n_{\text{jump}}) + TC)\varepsilon + (1 + h_k^{\max} L)B^i.$$

A discrete version of Gronwall's inequality (see, e.g., [28]) can be used to deduce

$$B^k \leq \frac{\exp(Lkh_k^{\max}) - 1}{L} \left(\left\| e^0 \right\|_X + (2M(1 + n_{\text{jump}}) + TC)\varepsilon \right).$$

The assertion

$$\sum_{t=0}^{k} h_t \left\| e^t \right\|_X \leq \frac{\exp(T_k' L) - 1}{L} \left(\left\| e^0 \right\|_X + (2M(1 + n_{\text{jump}}) + TC)\varepsilon \right)$$

follows immediately. ∎

The main differences compared to [17] are the following:

1. The explicit use of time steps h_t ensures temporal grid-independence of the result provided that the ratio of the largest to the smallest step size (and thus T_k') stays bounded. (We shall observe below that the constants, however, depend on the spatial grid.)
2. We explicitly take into account a finite number n_{jump} of discontinuities in the nonautonomous part of Φ, e.g., caused by jumps in the inflow profiles. To this end, we do not require (25) to hold for all $t \in I$ but accept n_{jump} violations of (25) at those t not in I'. These exceptions can be covered in the proof by enlarging the approximation constant by a term involving n_{jump}.
3. The initial offset δ^0 in (26), which is not present in [17], can be exploited in case we do not let ε go to zero.
4. We rephrased the assumptions so that no special choice for the norm $\|.\|_\Omega$ is required in the proof.

We now apply Lemma 1 to the following objects: We assume that we have obtained a relaxed solution $\boldsymbol{\omega}_t = \boldsymbol{\omega}_t^{\text{rlx}} \in \mathcal{H}, t = 0, \ldots, n_T$, of the Stage I NLP relaxation of (22). We then set $n = \sum_{i \in E}(n_L^i + 1), D = [0,1]^n$ and identify for $t = 0, \ldots, n_T - 1$

$$\begin{aligned} h_t &= \Delta t, & \Psi(t) &= \boldsymbol{\Psi}(t), & \Phi(t,y) &= \boldsymbol{\Phi}(t, y, \hat{\boldsymbol{\gamma}}_t, \bar{\boldsymbol{\gamma}}_t, \hat{\boldsymbol{h}}_t, \bar{\boldsymbol{h}}_t), \\ \alpha^t &= \boldsymbol{\omega}_t, & y^t &= \boldsymbol{\rho}_t, & y^{n_T} &= \boldsymbol{\rho}_{n_T}. \end{aligned}$$

In order to verify the remaining assumptions, we choose the maximum norm on $\mathbb{R}^{n_\Omega}$ for $\|.\|_\Omega$ and the discrete L^1-norm for densities $\boldsymbol{\rho}_t \in \mathbb{R}^n$ according to

$$\|\boldsymbol{\rho}_t\|_X = \sum_{i \in E} \sum_{k=0}^{n_L^i} \left| \rho_{k,t}^i \right| \Delta x^{(i)}.$$

We now determine an integer vector $\beta^t \in \mathcal{H} \cap \{0,1\}^{n_\Omega}$ as the solution of the Stage II mixed-integer linear program without dynamic constraints (the CIAP) [27],

$$\begin{aligned} &\min_{\substack{\beta^t \in \mathcal{H} \cap \{0,1\}^{n_\Omega}, \\ t=0,\ldots,n_T-1 \\ \delta^0 \in \mathbb{R}^{n_\Omega}, \varepsilon \in \mathbb{R}_{\geq 0}}} \varepsilon \\ &\text{subject to} \quad \left\| \delta^0 + \sum_{t=0}^{k-1} \Delta t(\boldsymbol{\omega}_t - \beta^t) \right\|_\Omega \leq \varepsilon \quad \text{for all } k = 0, \ldots, n_T. \end{aligned} \tag{28}$$

Here we exploit the fact that the upper bound on the norm $\|.\|_\Omega$ can be reformulated as a set of linear constraints. The objective is to minimize ε and thus the left-hand side

of assumption (26). Once the β^t have been determined from (28), the corresponding densities η^t can then be computed based on the iteration

$$\eta^0 = y^0, \quad \eta^{t+1} = \eta^t + \Delta t \Phi(t, \eta^t)\beta^t \quad \text{for } t = 0, \dots, n_T - 1.$$

It is well known that (28) can be solved in polynomial time and that its objective value ε is proportional to Δt [27]. Thus, Lemma 1 delivers that we can approximate the optimal relaxed densities of Stage I arbitrarily well by using the integer-feasible β^t instead of $\boldsymbol{\omega}^t$, provided that Δt is chosen small enough. We elaborate this discussion at the end of section 4.1.

We now check that Lemma 1 can indeed be applied. In order to show the bound (23), we arbitrarily choose $t \in I \cup \{n_T\}$, $y = \boldsymbol{\rho}_t \in D$, and $v \in \mathbb{R}^{n_\Omega}$ and observe that with $\Delta x_{\min} := \min_{i \in E} \Delta x^{(i)}$ and $\nu_{\max} = \max_{i \in E} \nu^{(i)}$ the bounds on $\rho^i_{t,k} \in [0,1]$ and $f(\rho) \in [0, f(\rho^*)]$ imply

$$\begin{aligned}
\|\Phi(t, \boldsymbol{\rho}_t)v\|_X &= \sum_{i \in E} \sum_{k=0}^{n_L^i} \left| \sum_{s=1}^{n_\Omega} \left(\nu^{(i)} \frac{\rho^i_{t,k-1} - 2\rho^i_{t,k} + \rho^i_{t,k+1}}{(\Delta x^{(i)})^2} \right.\right. \\
&\qquad \left.\left. + \frac{f^+_{s,i,k}(\rho^i_{t,k+1}, \rho^i_{t,k}, \hat{\gamma}^i_t) - f^-_{s,i,k}(\rho^i_{t,k}, \rho^i_{t,k-1}, \bar{\gamma}^i_t)}{2\Delta x^{(i)}} \right) v_s \right| \Delta x^{(i)} \\
&\leq \sum_{i \in E} \sum_{k=0}^{n_L^i} \left(\frac{4\nu^{(i)}}{(\Delta x^{(i)})^2} + \frac{2f(\rho^*)}{2\Delta x^{(i)}} \right) \sum_{s=1}^{n_\Omega} |v_s| \, \Delta x^{(i)} \\
&\leq \frac{4\nu_{\max} + f(\rho^*)\Delta x_{\min}}{\Delta x^2_{\min}} n_\Omega \left(\sum_{i \in E} L^i \right) \|v\|_\Omega =: M \|v\|_\Omega .
\end{aligned}$$

We now investigate the Lipschitz assumption (24). To this end, we additionally choose $\eta = \boldsymbol{\eta}_t \in D$ and $\alpha \in \mathcal{H}$. Let $L_f \geq 1$ denote the Lipschitz constant of the flow function f. We then obtain

$$\begin{aligned}
&\left| f^+_{s,i,k}(\rho_+, \rho_\circ, \hat{\gamma}) - f^+_{s,i,k}(\eta_+, \eta_\circ, \hat{\gamma}') \right| \leq 2L_f \left(|\rho_+ - \eta_+| + |\rho_\circ - \eta_\circ| + |\hat{\gamma} - \hat{\gamma}'| \right), \\
&\left| f^-_{s,i,k}(\rho_\circ, \rho_-, \bar{\gamma}) - f^-_{s,i,k}(\eta_\circ, \eta_-, \bar{\gamma}') \right| \leq 2L_f \left(|\rho_\circ - \eta_\circ| + |\rho_- - \eta_-| + |\bar{\gamma} - \bar{\gamma}'| \right).
\end{aligned} \tag{29}$$

Hence, we can deduce that

$$\begin{aligned}
&\|[\Phi(t, \boldsymbol{\rho}_t) - \Phi(t, \boldsymbol{\eta}_t)]\, \alpha\|_X \\
&= \sum_{i \in E} \sum_{k=0}^{n_L^i} \left| \sum_{s=1}^{n_\Omega} \left(\nu^{(i)} \frac{\rho^i_{t,k-1} - 2\rho^i_{t,k} + \rho^i_{t,k+1} - \eta^i_{t,k-1} + 2\eta^i_{t,k} - \eta^i_{t,k+1}}{(\Delta x^{(i)})^2} \right.\right. \\
&\qquad + \frac{1}{2\Delta x^{(i)}} \Big(f^+_{s,i,k}(\rho^i_{t,k+1}, \rho^i_{t,k}, \hat{\gamma}^i_t) - f^-_{s,i,k}(\rho^i_{t,k}, \rho^i_{t,k-1}, \bar{\gamma}^i_t) \\
&\qquad\qquad \left.\left. - f^+_{s,i,k}(\eta^i_{t,k+1}, \eta^i_{t,k}, \hat{\gamma}^i_t) + f^-_{s,i,k}(\eta^i_{t,k}, \eta^i_{t,k-1}, \bar{\gamma}^i_t) \Big) \right) \alpha_s \right| \Delta x^{(i)} \\
&\leq \frac{4\nu_{\max} + 2L_f \Delta x_{\min}}{\Delta x^2_{\min}} n_\Omega \|\boldsymbol{\rho}_t - \boldsymbol{\eta}_t\|_X =: L \|\boldsymbol{\rho}_t - \boldsymbol{\eta}_t\|_X .
\end{aligned}$$

We use (29) again to finally address assumption (25). It turns out that we must require the additional assumption that there exist constants $C_\gamma \in \mathbb{R}$ and $n_{\text{jump}} \in \mathbb{N}$

such that for all $\Delta t > 0$ and $i \in E$,

$$\left|\hat{\gamma}^i_{t+1} - \hat{\gamma}^i_t\right| + \left|\bar{\gamma}^i_{t+1} - \bar{\gamma}^i_t\right| \leq \Delta t C_\gamma \quad \text{for all } t \in I \text{ except for } n_{\text{jump}} \text{ exceptions.} \tag{30}$$

We can then deduce that

$$\begin{aligned}
&\left\| \left[\Phi(t+1, \boldsymbol{\rho}_{t+1}) - \Phi(t, \boldsymbol{\rho}_t)\right] v \right\|_X \\
&= \sum_{i \in E} \sum_{k=0}^{n^i_L} \left| \sum_{s=1}^{n_\Omega} \left(\nu^{(i)} \frac{\rho^i_{t+1,k-1} - 2\rho^i_{t+1,k} + \rho^i_{t+1,k+1} - \rho^i_{t,k-1} + 2\rho^i_{t,k} - \rho^i_{t,k+1}}{(\Delta x^{(i)})^2} \right.\right. \\
&\quad + \frac{1}{2\Delta x^{(i)}} \Big(f^+_{s,i,k}(\rho^i_{t+1,k+1}, \rho^i_{t+1,k}, \hat{\gamma}^i_{t+1}) - f^-_{s,i,k}(\rho^i_{t+1,k}, \rho^i_{t+1,k-1}, \bar{\gamma}^i_{t+1}) \\
&\quad \left.\left. - f^+_{s,i,k}(\rho^i_{t,k+1}, \rho^i_{t,k}, \hat{\gamma}^i_t) + f^-_{s,i,k}(\rho^i_{t,k}, \rho^i_{t,k-1}, \bar{\gamma}^i_t) \Big) \right) v_s \right| \Delta x^{(i)} \\
&\leq \sum_{i \in E} \sum_{k=0}^{n^i_L} \left| \sum_{s=1}^{n_\Omega} \left(\frac{\nu^{(i)} \Delta t}{(\Delta x^{(i)})^2} \left(\Phi^s_{k-1}(t, \boldsymbol{\rho_t}) - 2\Phi^s_k(t, \boldsymbol{\rho_t}) + \Phi^s_{k+1}(t, \boldsymbol{\rho_t}) \right) \right.\right. \\
&\quad + \frac{2L_f \Delta t}{2\Delta x^{(i)}} \left(\left|\Phi^s_{k+1}(t, \boldsymbol{\rho_t})\right| + 2\left|\Phi^s_k(t, \boldsymbol{\rho_t})\right| + \left|\Phi^s_{k-1}(t, \boldsymbol{\rho_t})\right| \right) \\
&\quad \left.\left. + \frac{2L_f}{2\Delta x^{(i)}} \left(\left|\hat{\gamma}^i_{t+1} - \hat{\gamma}^i_t\right| + \left|\bar{\gamma}^i_{t+1} - \bar{\gamma}^i_t\right| \right) \right) v_s \right| \Delta x^{(i)} \\
&\leq \Delta t \left(\frac{4\nu_{\max} M + 4L_f M \Delta x_{\min}}{(\Delta x_{\min})^2} + \frac{L_f C_\gamma n_\Omega}{\Delta x_{\min}} \right) \|v\|_\Omega \\
&=: \Delta t C \|v\|_\Omega
\end{aligned}$$

for all $t \in I$ except for n_{jump} exceptions.

For each spatial discretization, we thus obtain the required constants $M, L < \infty$, which grow with $\mathcal{O}(1/\min_{i \in E} \Delta x^{(i)})$, however, and are thus not fully grid independent.

Discussion of approximation properties. A computationally tractable algorithm that solves the traffic light optimization problem (9) with provable approximation guarantees is currently out of reach. Our proposed heuristic provides at least the following partial guarantee: For a semidiscretization in space with fixed $\Delta x^{(i)}$ and fixed positive artificial diffusion terms $\nu^{(i)}$, the integer gap between the relaxed Stage I nonlinear program and the mixed-integer nonlinear program consisting of the Stage I nonlinear program augmented by additional integer constraints on $\boldsymbol{\omega}^t$ can be made arbitrarily small by refinement of the temporal discretization. We need to keep in mind, however, that the solution of the Stage I nonlinear program with integer constraints does not necessarily approximate the original traffic light problem (9) in a mathematically strict sense, because we dropped the bilevel intersection flux maximization (14), because we added artificial diffusion to the dynamics, and because the constants needed in the assumptions of Lemma 1 are not bounded for $\Delta x^{(i)} \to 0$. The numerical results in section 5, however, show that our proposed heuristic is computationally tractable and delivers feasible points of the original problem with, albeit nonoptimal, satisfactorily high objective values.

4.2. Case II: Additional combinatorial constraints that couple over time. In the presence of upper and lower time limits T_{red} and T_{green} on red and green phases, we still perform steps 1–3 and 5. Only the reconstruction in step 4

changes slightly because we add the additional combinatorial constraints to CIAP (28) in Stage II (cf. [27]). They read as

$$\sum_{t=k+1}^{k+\left\lfloor \frac{T_{\text{red}}}{\Delta t} \right\rfloor + 1} \sum_{s \in \Omega} a^s \beta_s^t \geq 1 \qquad \text{for } k = 0, \ldots, n_T - \left\lfloor \tfrac{T_{\text{red}}}{\Delta t} \right\rfloor - 2,$$

$$\sum_{t=k+1}^{k+\left\lfloor \frac{T_{\text{green}}}{\Delta t} \right\rfloor} \sum_{s \in \Omega} a^s \beta_s^t \geq \sum_{s \in \Omega} a^s \left\lceil \tfrac{T_{\text{green}}}{\Delta t} \right\rceil \left(\beta_s^{k+1} - \beta_s^k \right) \quad \text{for } k = 0, \ldots, n_T - \left\lfloor \tfrac{T_{\text{green}}}{\Delta t} \right\rfloor - 1.$$

Because these constraints are linear, the CIAP is still a mixed-integer linear program and can be solved with standard solvers. However, they render the Stage II CIAP mixed-integer linear program much harder than in Case I without additional combinatorial constraints: While it can be shown [27] that CIAP (28) in Case I allows for a polynomial-time solution with optimal value $\varepsilon \leq \Delta t/2$, the Stage II CIAP mixed-integer linear program in the presence of additional combinatorial constraints is much harder to solve, and no a priori objective upper bounds on ε in terms of Δt can be given. The approximation Lemma 1 can still be invoked, but ε can no longer be driven to zero by reducing Δt. Thus, the integer optimality gap cannot be driven to zero either. In practice, however, the two-stage approach still produces useful answers for practical purposes; see section 5.

4.3. A note on degeneracy. From a practical optimization point of view, also the Stage I nonlinear program in relaxed POC form can be difficult to solve due to degenerate solutions. For instance, it is quite likely that in the optimal solution some of the traffic density values $\rho_{t,k}^i$ at the edge boundaries $k \in \{0, n_L^i\}$ attain the value ρ^* of maximum flow. In this case, several constraints of (13) are active and linearly dependent. Hence, the linear independence constraint qualification (LICQ) is not satisfied in the solution. However, LICQ is often needed to guarantee convergence of NLP solvers. For primal-dual interior-point methods (see, e.g., [29]), which are based on following a central path parameterized by some scalar $\mu \geq 0$, the existence of the central path at the solution $\mu = 0$ cannot be guaranteed by the implicit function theorem if the LICQ is violated. One needs to rely on implementation-specific heuristics in this case, which are, luckily, often highly efficient.

5. Numerical results. In this section we analyze the benefits of the POC approach for the nonlinear traffic light optimization problem in various aspects: We compare the efficiency of the two-stage heuristic (described in section 3.4) to other heuristic approaches for different road networks with various grid sizes and amounts of combinatorial dependencies (i.e., we optionally include bounds on switching times as described in section 4.2). Furthermore, we consider the optimization of the full nonlinear problem and discuss the benefits of POC formulations and heuristic initial solution guesses for warm-starts.

All computations are performed on a PC equipped with 8 GB RAM and an Intel Core i5-3470 CPU at 3.20 GHz. Continuous nonlinear optimization problems are solved with the open source interior-point optimizer Ipopt, version 3.12 [29]. For linear mixed-integer optimization we use either CPLEX, version 12.5 [16] or SCIP, version 3.2.0 [9, 1, 30, 21]. For solving nonlinear mixed-integer problems, we use Ipopt within SCIP.

5.1. Parameter settings and scenarios. In this paper, we restrict ourselves to the quadratic flow function

$$f(\rho) = \frac{v^{\max}}{\rho^{\max}} \cdot \rho \cdot (\rho^{\max} - \rho) \tag{31}$$

with $\rho^{\max} = 1$ and $v^{\max} = 1$. Obviously, f satisfies $f(0) = f(1) = 0$ and has a unique strict maximum $f(\rho^*) = \frac{1}{4}$ at $\rho^* = \frac{1}{2}$. In accordance with the CFL condition (15) we choose $\Delta t = \frac{1}{2}\Delta x^{(i)}$.

In what follows, we examine the following scenarios.

2 × 2-junction. We consider a 2 × 2-junction as shown in Figure 1.

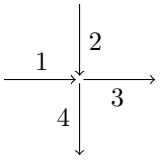

FIG. 1. *Network of a* 2 × 2*-junction.*

All roads have length $L_i = 1$. The initial traffic density is set to $\rho_0 = 0.1$, and the incoming boundary density is given as shown in Figure 2. The traffic distribution is 50% to road 3 and 50% to road 4 from each of the incoming roads, i.e., $d_{1,3} = d_{1,4} = d_{2,3} = d_{2,4} = 0.5$.

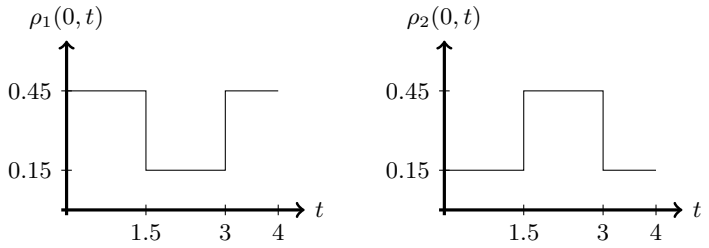

(a) Left boundary density of road 1. (b) Left boundary density of road 2.

FIG. 2. *Boundary density of incoming roads* 1 *and* 2.

8 × 4-junction. Furthermore, we consider a junction with eight traffic lights as presented in [12]; see Figure 3. Each of the four incoming roads splits into two lanes (left turn lane and straight/right turn lane) in front of the junction. Together with the four outgoing roads, the complete network consists of 16 edges (roads).

The incoming boundary flow and the road lengths L_i are set as in [12, p. 16]. The distribution of traffic at branching points is as follows for all four directions: 10% of the traffic goes to the left turning lane and 90% goes to the straight/right turning lane, from which 70% goes straight and 30% turns to the right.

For both scenarios, we consider a coarse discretization grid with grid sizes $\Delta t = 0.1$ and $\Delta x = 0.2$ as well as a finer discretization with $\Delta t = 0.05$ and $\Delta x = 0.1$. The time horizon is set to $T = 4$.

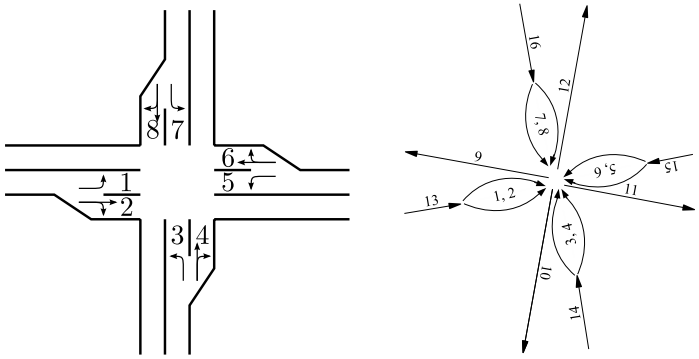

FIG. 3. *A traffic junction with eight traffic lights. Each lane is modeled by a separate edge.*

5.2. Two-stage heuristic with POC approach. We consider the heuristic strategy as described in section 4.

The relaxed nonlinear program obtained by POC (see section 3.4) yields a relaxed solution of the original traffic light optimization problem (9). In Stage I, we solve it with Ipopt.

In Stage II we use the ω-values of the obtained solution as input for CIAP which is then solved by a linear mixed-integer optimization solver. Here we use SCIP as well as CPLEX and compare the results. At this point we can optionally include the additional upper and lower bounds on red and green phases of traffic lights in CIAP, which we chose as $T_{\text{green}} = 0.3$ and $T_{\text{red}} = 3$.

As a last step we use the optimal traffic light setting obtained in Stage II and compute the forward solution (including the intersection flux maximization (14) left out in (21)) yielding the corresponding values for traffic density and flow of the original nonlinear traffic light optimization problem (9).

The optimal solution ω obtained in Stage I and the resulting optimal traffic light setting obtained after Stage II (on the one hand by the solver SCIP and on the other hand by the solver CPLEX) are shown in Figure 4 for the 2×2-junction for different grid sizes.

For the 2×2-junction scenarios, Ω has two elements. $\omega_1 = 1$ corresponds to the situation where traffic light 1 is green and traffic light 2 is red and vice versa for ω_2.

The results for all considered scenarios are shown in Table 1.

Table 1 does not show the objective function value (OFV) of the optimal solution of CIAP, but rather the OFV that the resulting traffic light setting would yield in the original problem (9). The "*" means that the solution process has been interrupted (after one hour). Hence, the resulting solution is not necessarily globally optimal for CIAP.

The optimal solution of CIAP is not unique. Depending on the parameter setting of the solvers, different solutions can be found. Different optimal solutions of CIAP do not necessarily yield the same OFV in the original problem. (That is why the OFVs obtained by SCIP and CPLEX differ most of the time from each other.) CPLEX solves the CIAP faster than SCIP in all cases; however, the solution found by SCIP leads in most cases to a better primal bound of the original problem.

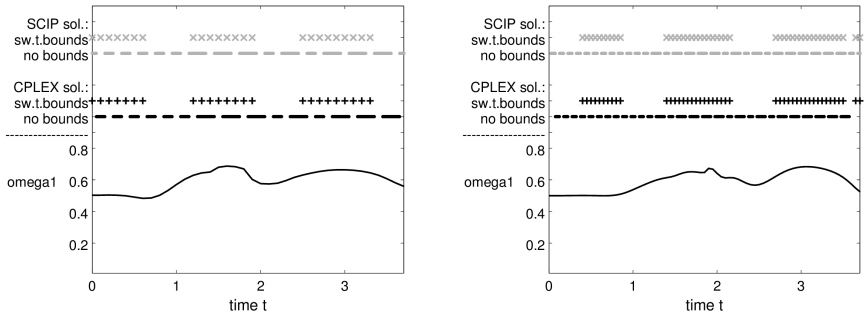

(a) Coarse grid size. (b) Fine grid size.

FIG. 4. *Results for road* 1 *in* 2×2*-junction. The first four lines show the time of the green phases of traffic light* 1 *using solver SCIP and CPLEX and regarding additional conditions on upper and lower bounds on switching times as described in section* 4.2. *The curve below shows* ω_1.

TABLE 1

Two-stage heuristic. We use the abbreviations vars *(number of variables),* OFV *(objective function value),* swt bnds *(presence of bounds on the switching times), and* fwd sol *(forward solution of the dynamics for given switching regime).*

Stage I			Stage II				
vars	OFV (Ipopt)	CPU time	swt bnds	vars of CIAP	solver	OFV of fwd sol	CPU time
2×2-junction coarse grid ($\Delta t = 0.1$)							
1704	3.6451	0.93s	no	161	SCIP	3.6467	2.16s
					CPLEX	3.6582	0.19s
			yes	83	SCIP	3.6118	0.32s
					CPLEX	3.6118	0.12s
2×2-junction fine grid ($\Delta t = 0.05$)							
5004	3.3948	5.70s	no	321	SCIP	3.4020	32.93s
					CPLEX	3.3851	2.31s
			yes	163	SCIP	3.3375	2.18s
					CPLEX	3.3373	0.68s
8×4-junction coarse grid ($\Delta t = 0.1$)							
7300	20.7062	91.35s	no	1281	SCIP	20.7657	12.82s
					CPLEX	20.7099	1.41s
			yes	657	SCIP	20.3205	>1h*
					CPLEX	20.2632	>1h*
8×4-junction fine grid ($\Delta t = 0.05$)							
20656	18.7653	675.78s	no	2561	SCIP	18.7817	423.42s
					CPLEX	18.7642	19.62s
			yes	1297	SCIP	18.0658	>1h*
					CPLEX	18.1359	>1h*

We can also observe that for both solvers, it is much harder to solve a problem which is highly combinatorially interconnected, even though it might have considerably less variables than another. For example, the CIAP for the 8×4-junction with additional restrictions on switching times is—even for the coarse grid ($\rightarrow$ 657 variables)—much harder to solve than the 8×4-junction without those restrictions for the fine grid ($\rightarrow$ 2561 variables).

5.3. MILP heuristic. Another possibility for obtaining heuristic solutions is to linearize problem (9). When we use a piecewise linear flow function as in [12], namely,

$$\tilde{f} = \begin{cases} \lambda \cdot \rho & \text{if } 0 \le \rho \le \rho^*, \\ \lambda \cdot (2\rho^* - \rho) & \text{if } \rho^* < \rho \le \rho^{\max} \end{cases} \tag{32}$$

with $\lambda = 0.5$, $\rho^* = 0.5$, and $\rho^{\max} = 1$ (cf. Figure 5), then we can apply various linearization techniques and solve the resulting mixed-integer linear program, for example, by CPLEX, as done in [12].

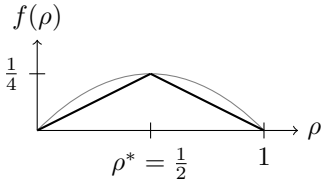

FIG. 5. *Piecewise linear vs. quadratic flow function.*

However, the dynamical behavior of the traffic using each of these flow functions differs considerably from one function to the other. A traffic density evolution of the 2×2-junction with even traffic light switching periods for both flow functions is shown in Figure 6. Hence, the optimal solution of the linearized version is not necessarily close to the optimal solution of the nonlinear model. However, we can use the resulting traffic light setting as a heuristic solution.

Now we compute optimal solutions of the mixed-integer linear program by CPLEX. Then, a forward simulation using the nonlinear flow function and also the intersection flow maximization condition (14) computes the corresponding OFV for the original flow problem.

The results are shown in Table 2. In comparison with Table 1, the MILP heuristic does not yield primal bounds that are as good as those of the two-stage heuristic. The only exception to this—where the MILP approach is better—is for the 8×4-junction with coarse discretization grid without restrictions on the switching times.

In Figures 7 and 8, the traffic light settings given by the two-stage heuristic (using CPLEX) and the MILP heuristic are shown. In Figure 7, no restrictions on the traffic lights are given. Here we can see that the left-turning lanes are kept red during the whole time horizon, since only a small percentage of the traffic is using it. If we add upper bounds for red phases (and lower bounds for green phases), this effect is avoided; see Figure 8.

In free traffic flow, that is, for $\rho < \rho^*$, the characteristic curves for the triangular flow functions are just parallel straight lines where the slope is independent of the incoming traffic (as long as $\rho < \rho^*$), so the characteristic curves cannot intersect. Even if the boundary density jumps to zero, the flow is determined by characteristic curves, as long as the outgoing flow is absorbed. In contrast to this, for the quadratic flow functions the characteristic curves are straight lines with different positive slopes depending on the incoming traffic, so intersections of the characteristic curves (that is, shocks) can easily occur after finite time, for example, for smooth but rapidly decreasing boundary densities. In this case one has to be careful in the boundary control if one wants to avoid shocks; see [13], in particular Example 10.

5.4. Optimizing nonlinear MIP with SCIP. Now we want to solve the complete nonlinear mixed-integer problem directly. SCIP is a solver that uses spatial

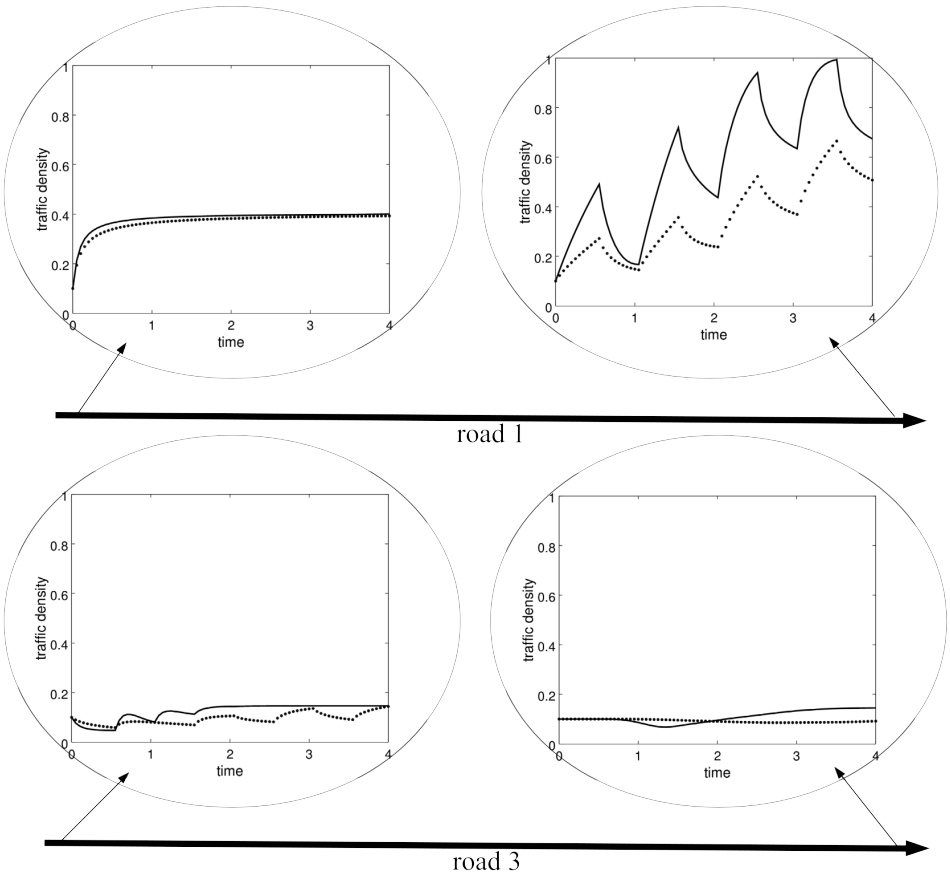

FIG. 6. *Comparison of traffic density evolution for different points of the traffic network. The black lines denote the traffic density using the smooth flow function* (31) *and the dotted lines denote the traffic density using the piecewise linear flow function* (32).

branch-and-bound for nonlinear constraints. In what follows, we consider two versions of the nonlinear MIP: one as stated in (9) and the other with outer convexification formulation as in (22). We consider again the option to include additional constraints for switching times. Since the problem has nonlinear constraints and integer variables and is highly combinatorially interconnected, it is extremely hard to solve.

As shown in Table 3, the solver is often not able to find any feasible solution within an hour if we do not provide a solution in the beginning. And even if the solver finds solutions by itself, in none of the cases does the primal bound exceed the heuristic solution found by the two-stage method, which in most cases obtains the solution much faster than in one hour (see Table 1).

When we provide the two-stage solution as incumbent for a warm-start, in none of the cases is SCIP able to improve this primal bound within the first hour.

Another observation is that the POC formulation seemingly leads to a slightly faster decrease of the dual bound. Hence, in most cases the duality gap after one hour is better than in the original problem formulation (9).

TABLE 2

MILP heuristic. We use the abbreviations vars *(number of variables),* OFV *(objective function value),* swt bnds *(presence of bounds on the switching times), and* fwd sol *(forward solution of the dynamics for given switching regime).*

Scenario	vars	swt bnds	OFV of fwd sol	time	gap
2×2 (coarse)	5740	no	3.4640	320.67s	0%
		yes	3.5039	3.98s	0%
2×2 (fine)	17820	no	3.2042	>1h	1.31%
		yes	3.2730	236.31s	0%
8×4 (coarse)	23616	no	20.7709	>1h	0.08%
		yes	out of memory		
8×4 (fine)	71280	no	18.6484	>1h	0.71%
		yes	out of memory		

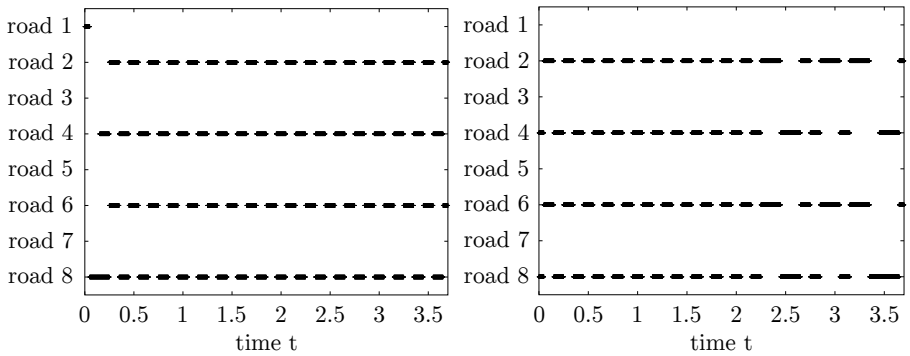

(a) Two-stage heuristic. (b) MILP heuristic.

FIG. 7. *The black bars denote the green phases of the corresponding traffic light.*

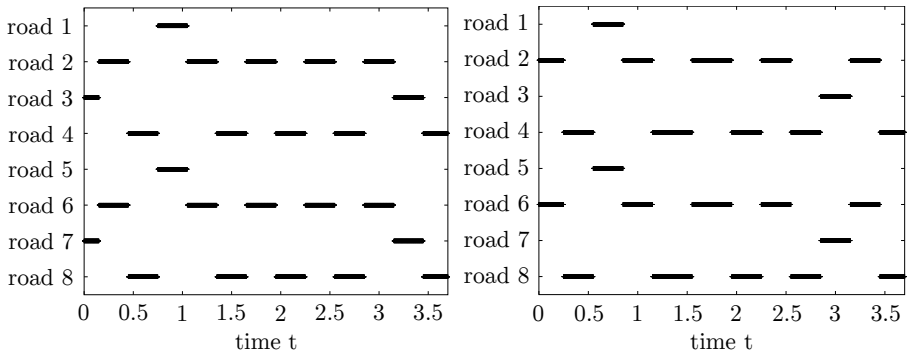

(a) Two-stage heuristic. (b) MILP heuristic.

FIG. 8. *Heuristic solution considering bounds on switching times. The black bars denote the green phases of the corresponding traffic light.*

6. Conclusion. For the traffic light optimization problem in [12], we proposed a solution heuristic consisting of five steps: Discretization, smoothing, solving a relaxed partial outer convexification (POC) nonlinear program with dynamic constraints (Stage I), reconstruction of a feasible mixed-integer solution from the combinatorial integer approximation problem (CIAP) mixed-integer linear program without dynamic

TABLE 3

Direct MINLP optimization with SCIP. We use the abbreviations POC *(formulation with partial outer convexification),* swt bnds *(presence of bounds on the switching times), and* OFV *(objective function value).*

POC	swt bnds	Start	Initial OFV	Best OFV after 1 hour	Dual bound after 1 hour	Gap
2×2-junction coarse grid ($\Delta t = 0.1$, 2369 variables)						
no	no	cold	–	3.6255	3.8172	5.29%
		warm	3.6582	3.6582	3.8262	4.59%
	yes	cold	–	3.5997	3.7829	5.09
		warm	3.6118	3.6118	3.8873	7.63%
yes	no	cold	–	3.6451	3.7622	3.21%
		warm	3.6582	3.6582	4.0421	10.49%
	yes	cold	–	3.6036	3.7143	3.07%
		warm	3.6118	3.6118	3.6817	1.94%
2×2-junction fine grid ($\Delta t = 0.05$, 7929 variables)						
no	no	cold	–	3.1937	3.7583	17.68%
		warm	3.4020	3.4020	3.7498	10.22%
	yes	cold	–	–	3.6759	$+\infty$
		warm	3.3375	3.3375	3.6680	9.90%
yes	no	cold	–	2.8932	3.6022	24.50%
		warm	3.4020	3.4020	3.6068	6.02%
	yes	cold	–	–	3.5181	$+\infty$
		warm	3.3375	3.3375	3.5242	5.59%
8x4-junction coarse grid ($\Delta t = 0.1$, 10601 variables)						
no	no	cold	–	8.9689	21.4075	138.69%
		warm	20.7657	20.7657	21.5964	4.00%
	yes	cold	–	–	21.5065	$+\infty$
		warm	20.3205	20.3205	21.5678	6.14%
yes	no	cold	–	–	21.3149	$+\infty$
		warm	20.7657	20.7657	21.2885	2.52%
	yes	cold	–	–	21.7347	$+\infty$
		warm	20.3205	20.3205	21.3367	5.00%
8x4-junction fine grid ($\Delta t = 0.05$, 33313 variables)						
no	no	cold	–	7.1245	19.7777	177.59%
		warm	18.7817	18.7817	19.7772	5.30%
	yes	cold	–	–	19.7772	$+\infty$
		warm	18.1359	18.1359	19.7772	9.05%
yes	no	cold	–	–	19.2470	$+\infty$
		warm	18.7817	18.7817	19.2470	2.48%
	yes	cold	–	–	19.1891	$+\infty$
		warm	18.1359	18.1359	19.1874	5.80%

constraints (Stage II), and, finally, a forward simulation to obtain a feasible solution candidate for the original problem. We prove a discrete approximation lemma that yields bounds on the quality of the Stage II solution with respect to the optimal CIAP objective function and some constants, which are independent of the time grid but dependent on the spatial grid. Numerical results indicate that the obtained solution candidates cannot be improved by global state-of-the-art mixed-integer nonlinear progamming (MINLP) methods within a reasonable amount of time. Furthermore, the two-stage solution candidates are better and usually faster to compute compared to global optima of piecewise linearized traffic flow models.

REFERENCES

[1] T. Achterberg, *SCIP: Solving constraint integer programs*, Math. Program. Comput., 1 (2009), pp. 1–41.

[2] E. Balas, *Disjunctive programming and a hierarchy of relaxations for discrete optimization problems*, SIAM J. Algebraic Discrete Methods, 6 (1985), pp. 466–486, https://doi.org/10.1137/0606047.

[3] C. Bardos, A. Y. le Roux, and J.-C. Nédélec, *First order quasilinear equations with boundary conditions*, Comm. Partial Differential Equations, 4 (1979), pp. 1017–1034.

[4] C. G. Claudel and A. M. Bayen, *Lax-Hopf based incorporation of internal boundary conditions into Hamilton-Jacobi equation. Part* I*: Theory*, IEEE Trans. Automat. Control, 55 (2010), pp. 1142–1157.

[5] G. M. Coclite, M. Garavello, and B. Piccoli, *Traffic flow on a road network*, SIAM J. Math. Anal., 36 (2005), pp. 1862–1886, https://doi.org/10.1137/S0036141004402683.

[6] B. Colson, P. Marcotte, and G. Savard, *An overview of bilevel optimization*, Ann. Oper. Res., 153 (2007), pp. 235–256.

[7] S. Dempe, *Bilevel programming*, in Essays and Surveys in Global Optimization, GERAD 25th Anniv. Ser. 7, C. Audet, P. Hansen, and G. Savard, eds., Springer, New York, 2005, pp. 165–193.

[8] G. Flötteröd and J. Rohde, *Operational macroscopic modeling of complex urban road intersections*, Transportation Res. Part B, 45 (2011), pp. 903–922.

[9] G. Gamreth et al., *The SCIP Optimization Suite* 3.2, ZIB-Report (15-60), Zuse Institute Berlin (ZIB), 2016, http://scip.zib.de/.

[10] M. Gerdts, *A variable time transformation method for mixed-integer optimal control problems*, Optimal Control Appl. Methods, 27 (2006), pp. 169–182.

[11] N. Geroliminis and A. Skabardonis, *Identification and analysis of queue spillovers in city street networks*, IEEE Trans. Intelligent Transportation Systems, 12 (2011), pp. 1107–1115.

[12] S. Göttlich, M. Herty, and U. Ziegler, *Modeling and optimizing traffic light settings in road networks*, Comput. Oper. Res., 55 (2015), pp. 36–51.

[13] M. Gugat, *Exact boundary controllability for free traffic flow with Lipschitz continuous state*, Math. Probl. Eng., 2016, 2743251.

[14] F. M. Hante, *Relaxation Methods for Hyperbolic PDE Mixed-Integer Optimal Control Problems*, preprint, 2015, https://arxiv.org/abs/1509.04052.

[15] F. M. Hante and S. Sager, *Relaxation methods for mixed-integer optimal control of partial differential equations*, Comput. Optim. Appl., 55 (2013), pp. 197–225.

[16] IBM Corporation, *IBM ILOG CPLEX Optimization Studio*, http://www-03.ibm.com/software/products/de/ibmilogcpleoptistud/ (31 January 2017).

[17] M. Jung, *Relaxations and Approximations for Mixed-Integer Optimal Control*, Ph.D. thesis, University of Heidelberg, 2013.

[18] M. Jung, C. Kirches, and S. Sager, *On perspective functions and vanishing constraints in mixed-integer nonlinear optimal control*, in Facets of Combinatorial Optimization, Springer, Heidelberg, 2013, pp. 387–417.

[19] M. N. Jung, G. Reinelt, and S. Sager, *The Lagrangian relaxation for the combinatorial integral approximation problem*, Optim. Methods Softw., 30 (2015), pp. 54–80.

[20] C. Kirches, S. Sager, H. G. Bock, and J. P. Schlöder, *Time-optimal control of automobile test drives with gear shifts*, Optimal Control Appl. Methods, 31 (2010), pp. 137–153.

[21] T. Koch, *Rapid Mathematical Programming*, Ph.D. thesis, TU Berlin, 2004.

[22] M. J. Lighthill and G. B. Whitham, *On kinematic waves.* II. *A theory of traffic flow on long crowded roads*, Proc. Roy. Soc. London Ser. A, 229 (1955), pp. 317–345.

[23] D. Ma, D. Wang, Y. Bie, and S. Di, *A method of signal timing optimization for spillover dissipation in urban street networks*, Math. Probl. Eng., 2013, 580546.

[24] G. F. Newell, *A simplified theory of kinematic waves in highway traffic*, Transportation Res. Part B, 27 (1993), pp. 281–313.

[25] P. I. Richards, *Shock waves on the highway*, Oper. Res., 4 (1956), pp. 42–51.

[26] S. Sager, H. G. Bock, and M. Diehl, *The integer approximation error in mixed-integer optimal control*, Math. Program., 133 (2012), pp. 1–23.

[27] S. Sager, M. Jung, and C. Kirches, *Combinatorial integral approximation*, Math. Methods Oper. Res., 73 (2011), pp. 363–380.

[28] J. Stoer and R. Bulirsch, *Introduction to Numerical Analysis*, 3rd ed., Texts Appl. Math. 12, translated from the German by R. Bartels, W. Gautschi, and C. Witzgall, Springer-Verlag, New York, 2002.

[29] A. Wächter and L. T. Biegler, *On the implementation of an interior-point filter line-search algorithm for large-scale nonlinear programming*, Math. Program., 106 (2006), pp. 25–57.

[30] R. Wunderling, *Paralleler und objektorientierter Simplex-Algorithmus*, Ph.D. thesis, TU Berlin, 1996.